Deep Learning-Based Risk Assessment of Depression Disease

Tushar Mehrotra[1], Bhawna Wadhwa[2], Mahalakshmi[3], Manish kumar Goyal[4]

Abstract: Millions of people all around the world are affected by depression, a prevalent mental health disease. Effective treatments and assistance depends on the early identification and precise risk assessment of depression. In this study, we provide a unique tuna swarm-optimized attention-based long/short-term memory (TSO-ALSTM) approach based on deep learning (DL) to estimate the risk of depression. The attention mechanism helps the model concentrate on key features, and LSTM is renowned for its capacity to simulate long-term reliance on sequential information. The model's performance is enhanced by using the TSO method to optimize its settings. We make use of a dataset gathered from a Kaggle source to determine the risk of depression. Based on the suggested TSO-ALSTM approach, a number of performance metrics, including AUC, precision, accuracy, recall, and f1-score, are examined in relation to the risk assessment of depression disorder. Results from experiments show how well the suggested TSO-ALSTM model performs in correctly estimating the probability of depression. In regards to accurate forecasting and the value of features, it performs better than other models and conventional machine learning techniques.

Keywords: Depression, risk assessment, deep learning (DL), tuna swarm optimized attention-based long/short-term memory (TSO-ALSTM)

1. Introduction

Depression is a complex and widespread mood disease that affects millions of people worldwide. It is frequently called the "common cold" of mental health. It is a severe condition marked by enduring depressive and gloomy feelings and losing interest or enjoyment in once-pleasant activities [1, 2]. Depression is a chronic illness that goes beyond passing feelings of melancholy and can negatively influence a person's emotional health, social interactions, and general quality of life. The complexity of depression, which includes various symptoms and causes, is one of its distinguishing characteristics. Although it is frequently considered a mental health condition, it can also cause physical symptoms such as changes in food, sleep habits, and energy levels [3]. Depression results from a complex combination of biological, psychological, and environmental elements rather than just being the result of personal weakness or a lack of motivation. Depression involves abnormalities in brain chemistry and neurocircuitry from a biological perspective. Serotonin, norepinephrine, and dopamine are neurotransmitters that govern mood. When these neurotransmitters are out of balance, emotional regulation problems can result. The risk of depression can also be influenced by a person's family history and genetic predispositions [4]. To create efficient interventions and treatments, it is essential to comprehend the neurological foundations of depression. Depressive disorders are also significantly influenced by psychological variables [5].

Rumination and self-criticism are negative mental processes that can feed and amplify depressed symptoms. Depression may start due to traumatic experiences, continuous chronic pressures, or stressful life events. The condition may also be more likely to develop in people with specific personality features like low self-esteem or a negative outlook. Givingpeople complete depression care means addressing these psychological issues. When comprehending depression, the importance of environmental influences shouldn't be understated. Depressive symptoms can persist due to social isolation, a lack of social support, and damaged relationships. Socioeconomic variables like poverty, unemployment, or traumatic childhood events can increase depression risk [6]. To encourage recovery and prevent relapse, it is crucial to identify and deal with these outside factors. It is imperative to approach sadness with empathy, comprehension, and a multifaceted viewpoint. Due to the intricacy of this condition, treatment must be comprehensive and may include a mix of psychotherapy, medication, lifestyle modifications, and support from loved ones. A person's prognosis and quality of life can be greatly enhanced by prompt intervention and early

[1]*Assistant Professor, College of Computing Science and Information Technology, Teerthanker Mahaveer University, Moradabad, Uttar Pradesh, India, Email id: tushar.cs17@nitp.ac.in*

[2]*Assistant Professor, Department of Data Science (CS), Noida Institute of Engineering and Technology, Greater Noida, Uttar Pradesh, India, Email id: bhawna.wadhwa@niet.co.in*

[3]*Professor Department of Computer Science and Engineering, Presidency University, Bangalore, India, Email Id: mahalakshmi@presidencyuniversity.in*

[4]*Assistant Professor, Department of Computer Science & Application, Vivekananda Global University, Jaipur, India, Email Id: manish.kumar.goyal@vgu.ac.in*

symptom diagnosis [7].To estimates the risk of depression, we provide a TSO-ALSTM based on deep learning (DL). The model is assisted in focusing on key features by the attention mechanism, and LSTM is renowned for its ability to simulate long-term reliance on sequential information. By optimizing the model's settings using the TSO method, performance is improved.

The remainder of this paper is arranged as follows: Part 2-related work, part 3- methodology, Part 4- results, and Part 5- conclusion with limitations and future scope.

2. Related Works

Machine Study [8] introduced the Context-DNN technique using multiple regression to forecast the risk of depression. Depression context data was used in developing the context-DNN technique, which combines context and DNNs to predict the beginning and extent of depression better.Article [9] developed prediction models using deep learning to evaluate the efficacy of antidepressant medication for patients in Taiwan.To automate the diagnosis of Parkinson's disease with electroencephalogram (EEG) recordings, a thirteen-layer CNN model was presented [10].Paper[11] proposed an EEG-based depression detection technique. In this approach, the framework of CNN, which is strong at extracting local characteristics, is combined with an LSTM network, which is good at learning long-term dependencies. EEG recordings of both the right and left hemispheres of 30 people are used to train the suggested CNN-LSTM system.

Study [12] presented a "CNN+Fuzzy logic model" for automatically diagnosing depressive states with a spatiotemporal representational framework. To better predict depressive episodes, the suggested FFL uses a DLN to combine spatial and temporal data.Research [13] predicts and forecasts the DBS pattern using Long Short Term Memory, a recurrent NN. The extent of neurological conditions is measured by analyzing the "rest tremor velocity (RTV)." They researched and analyzed RTV values to inform the network's architecture and training. To mimic and categorize diverse assault techniques, the DBS architecture includes several attack patterns.Article [14] suggested that the CNN approach could be used in a system for identifying EEG pathology. The EEG signals were pre-processed, and the CNN approach was given the resulting spatiotemporal representation. The "AlexNet deep CNN" was studied with a shallow CNN approach. Using the multilayer perceptron (MLP), they were able to fuse the CNN characteristics of three time-varying portions of the EEG signal.A study [15] suggested a novel DL technique called "Greedy Deep Weighted Dictionary Learning (GDWDL)" for the classification of mobile multi-media used in the diagnosis of medical conditions.

Data from patients' follow-up observations can be shared and analyzed using mobile multi-media technologies.

3. Method

3.1 Dataset

The "Beck Depression Inventory (BDI)" was employed for this research, and its dataset includes 23 questionnaires with six possible responses. Kaggle, an open platform for diagnosing depression disorder, provided the most recent, authentic BDI data. In total, there are 1403 samples in the dataset. The options for answers are presented in descending order of positivity. The relative importance of each choice is quantified. There are four possible answers, the first of which has the highest positive answer (0), while the other three tend towards the most negative solution (1, 2, and 3). A negative response of 3 is the strongest possible negative response to a question. The test consists of 23 questions, the numerical weights of which are summed together at the end. And the total of all the factors is used to determine the grade. Table 1 provides a range of values against which an evaluation can be conducted, allowing the severity of the disease to be calculated.

Table 1: BDI rating scale.

Grade (Depression)	Minimal	Mild	Moderate	Severe
Total	0-08	09-15	16-28	29-62
Condition	No Depression		Have Depression	

3.2 Data pre-processing

3.2.1 Min-max normalization

It is a widely used data pre-processing tool most data mining systems use. A dataset should be normalized by adjusting the values of each attribute so that they are all contained within a narrow range, such as 0.0 to 1.0. The min-max normalization strategy is used to pre-process child data and estimate the risk of malnutrition. The features or outputs are scaled using this method from one set of values to another. It is common to rescale the properties between $[0, 1]$ and $[-1, 1]$ or somewhere in between. The rescaling in Equation (1) is frequently performed using a formula for linear interpretation, such as

$$z' = \frac{z - min_F}{max_F - min_F}(new\_max_F - new\_min_F) + new\_min_F$$
(1)

Where max_F is the attribute's highest value, min_F is its lowest value, and $(new\_max_F - new\_min_F) = 0$. When $max_F - min_F = 0$, It implies that the data's value for that particular feature is constant. Each component will remain the same after applying the min-max normalization if it

falls within the new range of values.

3.3 Long/short-term memory (LSTM)

In this research, we conducted experiments with LSTM. Three gates, the forget gate e_s, the input gate g_{s-1}, and the output gate w_s, regulate LSTM once a cell state has been introduced. The LSTM cell status will determine which information should be remembered and deleted. The LSTM model structure is presented in Figure 1.
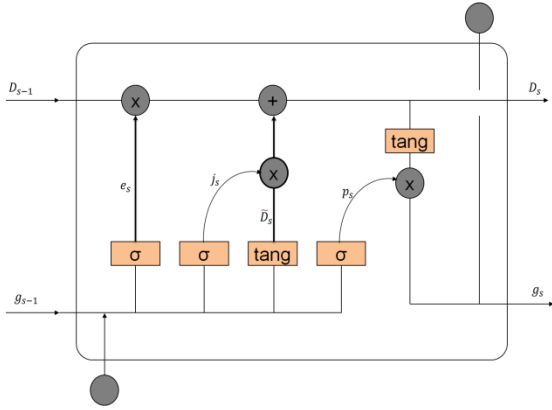
Figure 1: LSTM structure

In LSTM, the initial step is determining what data from the cell state may be safely discarded. Last-second input (w_s) and the concealed state (g_{s-1}) are used to determine the forget gate (e_s). The Equation is as follows:

$$e_s = \sigma(X_e \cdot [g_{s-1}, w_s] + a_e)$$
(2)

The next stage is to settle on what new data should be added to the current state of the cell. The first step is to determine what data needs to be refreshed. To determine the input gate (j_s), we plug in g_{s-1} and w_s. The Equation is as follows:

$$j_s = \sigma(X_j \cdot [g_{s-1}, W_s] + a_j)$$
(3)

Then, using g_{s-1} and w_s, we can determine the temporary state of the cell $(\widetilde{D}_s)$, which may be added to the cell data. The Equation is as follows:

$$\widetilde{D}_s = tang(X_d \cdot [g_{s-1}, w_s] + a_c)$$
(4)

e_s, j_s, and the previous cell state (D_{s-1}) are used to get the current cell state (D_s). The Equation is as follows:

$$D_s = e_s * D_{s-1} + j_s * \widetilde{D}_s$$
(5)

After the state of the cell has been updated, g_{s-1} and w_s are used to determine the output gate (p_s). Specifically, here is the Equation:

$$p_s = \sigma(X_p \cdot [g_{s-1}, w_s] + a_p)$$
(6)

At last, p_s and D_s derive the current concealed state (g_s). Here is the Equation:

$$g_s = p_s * tang(D_s)$$
(7)

X_e, X_j, X_d, X_p and Xp are the weights matrix, and $a_e, a_j, a_d, a_{nd\,ap}$ are the associated bias in the formula. Tang: activation function; σ: sigmoid activation functions.

3.4 Attention Mechanism

In this research, we extend the LSTM model to include an attention mechanism, and we employ the LSTM-Attention model to identify depression disease. The LSTM's hidden layer is where the attention is added, with the fully connected layer translating the hidden state (g_s) into the desired attention weight (v_s). The Equation is as follows:

$$v_s = tang(g_s)$$
(8)

For attention probability measures, thesoftmax function produces values $b_1, b_2, b_3 \cdots, and\ b_s$ for the attention probability distribution. The Equation is as follows:

$$b_s = \frac{\exp(v_s)}{\sum_{s=1}^n \exp(v_s)}$$
(9)

Emphasis weighting distribution, Based on b_s and g_s, a context vector v can be determined. The Equation is as follows:

$$u = \sum_{s=1}^n b_s \cdot g_s$$
(10)

3.5 Attention-based long short term memory (ALSTM)

We analyze the current NN model to develop a network detection model based on LSTM-Attention to increase the accuracy rate of depression prediction. The structure of ALSTM is shown in Figure 2.

➢ Input layer: For instance, consider a sample of experimental data. Once data has been tokenized, it is represented initially by vectors $w_1, w_2, w_3 \cdots, w_s$. In this stage, the embedding layer is not employed because it is unnecessary following the completion of the data vector matrix embedding training in the data pre-processing phase.

➢ LSTM layer: The output of the matching hidden layer $g_1, g_2, g_3, \cdots, g_s$ can be obtained by feeding each input into the LSTM unit in this layer. Automatically learning the characteristics of depression detection, it employs LSTM to address the issue of long-term dependencies.

➢ Attention layer: We use the hidden layer's attention system to calculate the attention probability distribution values $b_1, b_2, b_3 \cdots, b_s$

➢ Dropout layer: Overfitting is prevented with dropout technology in this layer
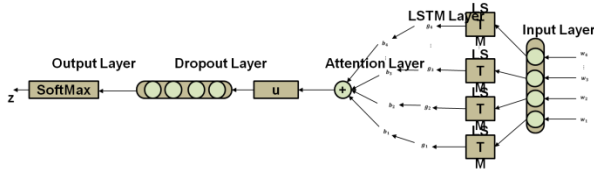
Fig 2: TSO-ALSTM structure

3.6 Tuna Swarm Optimization (TSO)

3.6.1 Initialization

To begin the optimization process, TSO, like other swarm-based algorithms, randomly generates starting populations distributed uniformly across the search space,

$$W_j^{int} = rand \cdot (ub - 1b) + 1b, j = 1,2,\cdots, MO, \quad (11)$$

Where W_j^{int} is the jth represents the starting member of group B, ub, and $1b$ define the search space's boundaries at both ends. NP represents "the total number of tuna populations, and the rand is a uniformly distributed random vector" from 0 to 1.

3.6.2 Spiral Foraging

When small schooling fish such as "sardines, herring, and others encounter predators," they form a thick structure and move in various directions simultaneously. This makes it hard for the predators to hold on to a specific target. The School of Tuna pursues its target by establishing a tight spiral shape. Most fish in a school has a poor sense of direction, but when a few swim confidently in one order, the rest of the school will follow suit until they've all aligned on a single course and are ready to hunt. Schools of tuna do more than just spiral after prey; they also share knowledge. The tunas can share knowledge with their neighbors because they all follow the same pattern of behavior. The following is a mathematical equation for the spiral foraging method, which is based on the previous strategy:

$$W_j^{s+1} =$$
$$\begin{cases} \alpha_1 \cdot (W_{best}^s + \beta \cdot |W_{best}^s - W_j^s|) + \alpha_2 \cdot W_j^s, \ i = 1, \\ \alpha_1 \cdot (W_{best}^s + \beta \cdot |W_{best}^s - W_j^s|) + \alpha_2 \cdot W_{j-1}^s, i = 2,3,\cdots, MO \end{cases}$$
$$(12)$$

$$\alpha_1 = b + (1-b) \cdot \frac{s}{s_{max}} \quad (13)$$

$$\alpha_2 = (1-b) - (1-b) \cdot \frac{s}{s_{max}} \quad (14)$$

$$\beta = f^{ak} \cdot \cos(2\pi a), \quad (15)$$

$$k = f^{3cos}(((s_{max} + 1/t) - 1)\pi), \quad (16)$$

In this Equation, A is the B individual in the C iteration, D is the present optimal individual, F and A1 are the coefficients of weight that regulate the inclination of people to advance towards the optimal and the prior individual, respectively. t is the present iteration number, A3 is the greatest number of iterations, and b is an evenly distributed random number that ranges from 0 to 1. A2 is a constant that controls how closely the tuna initially follow the optimal individual and the prior individual.

The tuna has a high capacity for exploiting the search region around the food when they all forage in a spiral pattern. Blindly following the optimal individual to feed is not helpful for group foraging if the optimal individual has been unsuccessful in locating food. This leads us to consider using a randomly generated coordinate in the search space as a starting point for the spiral search algorithm. That way, people can look at many places simultaneously, and TSO can explore the entire planet. This particular mathematical structure is defined as follows:

$$W_j^{s+1} =$$
$$\begin{cases} \alpha_1 \cdot (W_{rand}^s + \beta \cdot |W_{rand}^s - W_j^s|) + \alpha_2 \cdot W_j^s, \ i = 1, \\ \alpha_1 \cdot (W_{rand}^s + \beta \cdot |W_{rand}^s - W_j^s|) + \alpha_2 \cdot W_{j-1}^s, \ i = 2,3,\cdots, MO \end{cases}$$
$$(17)$$

Where A1 rand is generated at a random starting point within the search space, metaheuristic algorithms are known for their tendency to first conduct a broad sweep of the area before shifting gears to focus on local optimization. When TSO continues to iterate, the referring points of spiral foraging turn the random individuals into ideal individuals. A complete mathematical representation of the spiral foraging approach is as follows:

$$W_j^{s+1}$$
$$= \begin{cases} \begin{cases} \alpha_1 \cdot (W_{rand}^s + \beta \cdot |W_{rand}^s - W_j^s|) + \alpha_2 \cdot W_j^s, \ i = 1, \\ \alpha_1 \cdot (W_{rand}^s + \beta \cdot |W_{rand}^s - W_j^s|) + \alpha_2 \cdot W_{j-1}^s, \ i = 2,3,\cdots, MO \end{cases}, & if \ rand < \frac{s}{s_{max}} \\ \begin{cases} \alpha_1 \cdot (W_{best}^s + \beta \cdot |W_{best}^s - W_j^s|) + \alpha_{z2} \cdot W_j^s, \ i = 1, \\ \alpha_1 \cdot (W_{best}^s + \beta \cdot |W_{best}^s - W_j^s|) + \alpha_2 \cdot W_{j-1}^s, \ i = 2,3,\cdots, MO \end{cases}, & if \ rand \geq \frac{s}{s_{max}} \end{cases}$$

(18)

3.6.3 Parabolic Foraging

When feeding, tunas form a spiral shape but also "a parabolic cooperative feeding" pattern. Using a plate of food as a pivot point, tuna produces a parabolic shape. When hungry, tuna look for food in their immediate environment. Both methods are used simultaneously because each has a 50% chance of being chosen. SE is a random number between 0 and 1. Details of the underlying mathematical framework are as follows:

$$W_j^{s+1} = \begin{cases} W_{best}^s + rand \cdot (W_{rand}^s - W_j^s) + SE \cdot o^2 \cdot (W_{rand}^s - W_j^s), & if \ rand < 0.5, \\ SE \cdot o^2 \cdot W_j^s, & if \ rand \geq 0.5, \end{cases} \quad (19)$$

$$o = \left(1 - \frac{s}{s_{max}}\right)^{\left(\frac{s}{s_{max}}\right)}, \quad (20)$$

4. Result and Discussion

BDI models were developed using various approaches and procedures to diagnose depressive disorder, and the results were analyzed.Where "true positives (S_1), false positives (I_1), true negatives (S_2), and false negatives (I_2)" Depression diagnosis Performance comparison of methodsis presented in Table2.

Table 2: Methods comparison

Model	Accuracy (%)	Precision (%)	Recall (%)	F1-measure (%)	AUC (%)
Naive Bayes [16]	96.50	93.60	93.60	93.60	98.60
Decision Tree [16]	92.80	87.10	87.20	87.10	90.80
Neural Network [16]	98.70	98.50	98.40	98.40	99.90
Random Forest [16]	94.80	90.40	90.40	90.30	96.60
TSO-ALSTM [Proposed]	99.20	99.40	98.90	99.10	99.95

Accuracy is the degree to which a computation or estimation corresponds to the actual or true value. It is a significant statistic in evaluating predictive models, as in Equation (21).Figure3 depicts the accuracy comparison for existing Naive Bayes [16], Decision Tree [16],Neural Network [16], and Random Forest [16] is 85%, 78%, 25%, and 83%, and our proposed approach TSO-ALSTM has99.20%. It shows that our proposed method is more accurate in predicting depression diagnosis than the existing techniques.

$$Accuracy = \frac{S_2 + S_1}{S_2 + S_1 + I_2 + I_1} \quad (21)$$
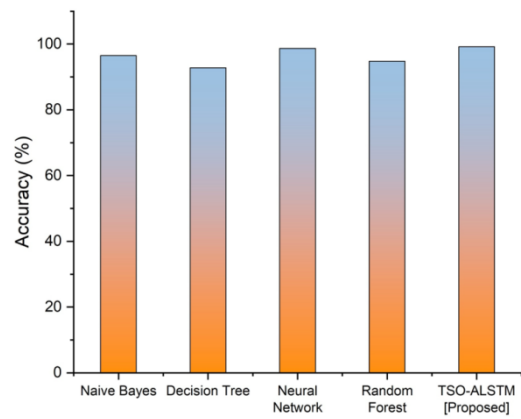
Fig 3: Accuracy

The ratio of the number of positive samples that may be anticipated to the number of positive samples which can be reliably predicted is the factor that defines the precision of the test as in Equation. (22). Figure 4 depicts a precision comparison of existing and proposed approaches. The existing approachesexisting Naive Bayes [16], Decision Tree [16], Neural Network [16], and Random Forest [16] are 93.6%, 87.1%, 98.5%, and 90.4%, and our proposed TSO-ALSTMhas 99.40%. It illustrates that our proposed technique is higher in precision.

$$Precision = \frac{S_1}{S_1 + I_1} \quad (22)$$
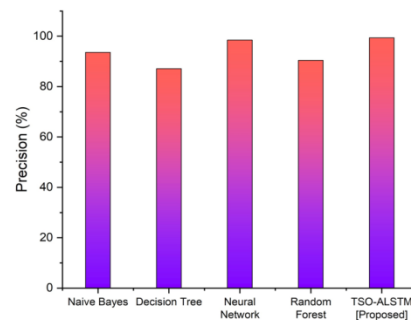
Fig 4: Precision

Calculating recall involves comparing the total number of positive samples which were properly predicted to the number of samples that were accessible in that class. This provides the percentage that is used in the calculation of recall as in Equation. 23.Figure 5 displays the performance of recall for Naive Bayes [16], Decision Tree [16], Neural Network [16], and Random Forest [16] is93.6%, 87.2%, 98.4%, and 90.4% and the proposed approach TSO-ALSTM is 98.90%.It can be conclude that the proposed method achieves the greatest recall rate than other methods.

$$Recall = \frac{S_1}{S_1 + I_2} \quad (23)$$
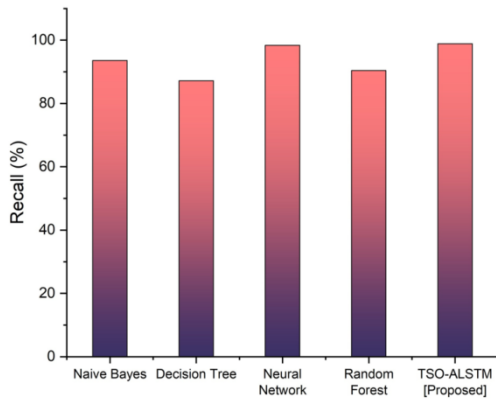
Fig 5: Recall

F1-measure is the average value of recall and precision as in Equation (24). The recall comparison for existing and proposed approaches is shown in Figure 6. The existing approaches Naive Bayes [16], Decision Tree [16], Neural Network [16], and Random Forest [16] is 93.6%, 87.1%, 98.5%, and 90.3%, and the proposed technique TSO-ALSTM have value of 99.10%. Compared to other methods, the proposed approach achieves the highest F1-measure rate.

$$F1 - measure = \frac{2 \times (Presicion \times Recall)}{Presicion + Recall}$$
(24)
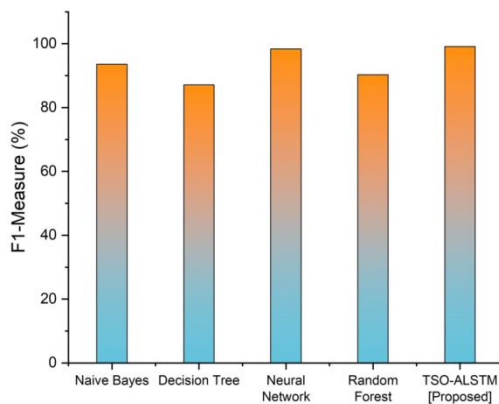
Fig 6: F1-measure

Area under the curve (AUC) quantifies the total value within an interval, often representing aggregated data, probability, or other cumulative measures over time/distance. Figure 7 displays the performance of recall for Naive Bayes [16], Decision Tree [16], Neural Network [16], and Random Forest [16] is98.6%, 90.8%,99.90%, and 96.6% compared with the proposed approach TSO-ALSTM is 99.95%. The proposed method has the highest AUC rate compared to other methods.
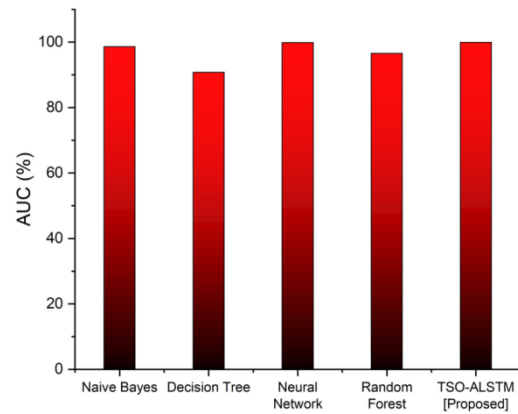
Fig 7: AUC comparison

5. Conclusion

Nowadays, the BDI is frequently used to gauge the diagnosis and severity of depression. In this research, we presented a novel deep learning (DL)-based tuna swarm-optimized attention-based long/short-term memory (TSO-ALSTM) approach for predicting the risk of depression. For this study, the "Beck Depression Inventory (BDI)" was used, and its dataset consists of 23 questionnaires with six possible answers. The most recent, accurate BDI data was provided by Kaggle, an open platform for diagnosing depression disorder. The Values of performance metrics for our proposed method were obtained in terms of accuracy (99.20%), precision (99.40%), recall (98.90%), f1-measure (99.10%), and AUC (99.95). The TSO-ALSTM approach is designed specifically for risk estimation of depression. It may not easily adapt to other tasks or domains without significant modifications or retraining. Further investigation is needed to determine how well various constraint-handling strategies handle constrained optimization issues.

References

[1] Rensma, S.P., van Sloten, T.T., Launer, L.J. and Stehouwer, C.D., 2018. Cerebral small vessel disease and risk of incident stroke, dementia and depression, and all-cause mortality: a systematic review and meta-analysis. Neuroscience &Biobehavioral Reviews, 90, pp.164-173.

[2] Tully, P.J., Ang, S.Y., Lee, E.J., Bendig, E., Bauereiß, N., Bengel, J. and Baumeister, H., 2021. Psychological and pharmacological interventions for depression in patients with coronary artery disease. Cochrane Database of Systematic Reviews, (12).

[3] A T.G., Lee, H.S., Park, S.W. and Seon, H.C., 2020. Effect of Nordic walking on depression and physical function in the elderly with high-risk of depression. Korean Society of Physical Medicine, 15(4), pp.11-20.

[4] March, C., Huscher, D., Preis, E., Makowka, A., Hoeppner, J., Buttgereit, F., Riemekasten, G., Norman, K. and Siegert, E., 2019. Prevalence, risk factors and assessment of depressive symptoms in patients with systemic sclerosis. Archives of rheumatology, 34(3), p.253.

[5] Ko, J.Y., Rockhill, K.M., Tong, V.T., Morrow, B. and Farr, S.L., 2017. Trends in postpartum depressive symptoms—27 states, 2004, 2008, and 2012. Morbidity and Mortality Weekly Report, 66(6), p.153.

[6] Yao, Y., Ding, G., Wang, L., Jin, Y., Lin, J., Zhai, Y., Zhang, T., He, F. and Fan, W., 2019. Risk factors for depression in empty nesters: a cross-sectional study in a coastal city of Zhejiang Province and China. International journal of environmental research and public health, 16(21), p.4106.

[7] Thomas, E. and Seedat, S., 2018. The diagnosis and management of depression in the era of the DSM-5. South African Family Practice, 60(1), pp.22-28.

[8] Baek, J.W. and Chung, K., 2020. Context deep neural network model for predicting depression risk using multiple regression. IEEE Access, 8, pp.18171-18181.

[9] Lin, E., Kuo, P.H., Liu, Y.L., Yu, Y.W.Y., Yang, A.C. and Tsai, S.J., 2018. A deep learning approach for predicting antidepressant response in major depression using clinical and genetic biomarkers. Frontiers in psychiatry, 9, p.290.

[10] Oh, S.L., Hagiwara, Y., Raghavendra, U., Yuvaraj, R., Arunkumar, N., Murugappan, M. and Acharya, U.R., 2020. A deep learning approach for Parkinson's disease diagnosis from EEG signals. Neural Computing and Applications, 32, pp.10927-10933.

[11] Ay, B., Yildirim, O., Talo, M., Baloglu, U.B., Aydin, G., Puthankattil, S.D. and Acharya, U.R., 2019. Automated depression detection using deep representation and sequence learning with EEG signals. Journal of medical systems, 43, pp.1-12.

[12] Rajawat, A.S., Bedi, P., Goyal, S.B., Bhaladhare, P., Aggarwal, A. and Singhal, R.S., 2023. Fusion Fuzzy Logic and Deep Learning for Depression Detection Using Facial Expressions. Procedia Computer Science, 218, pp.2795-2805.

[13] Rathore, H., Al-Ali, A.K., Mohamed, A., Du, X. and Guizani, M., 2019. A novel deep learning strategy for classifying different attack patterns for deep brain implants. IEEE Access, 7, pp.24154-24164.

[14] Alhussein, M., Muhammad, G. and Hossain, M.S., 2019. EEG pathology detection based on deep learning. IEEE Access, 7, pp.27781-27788.

[15] Wu, C., Luo, C., Xiong, N., Zhang, W. and Kim, T.H., 2018. A greedy deep learning method for medical disease analysis. IEEE Access, 6, pp.20021-20030.

[16] Butuner, R. and Yuksel, H., 2021. Diagnosis and Severity of Depression Disease in Individuals with Artificial Neural Networks Method. International Journal of Intelligent Systems and Applications in Engineering, 9(2), pp.55-63.

[17] Mr. Dharmesh Dhabliya, Ms. Ritika Dhabalia. (2014). Object Detection and Sorting using IoT. International Journal of New Practices in Management and Engineering, 3(04), 01 - 04. Retrieved from http://ijnpme.org/index.php/IJNPME/article/view/31

[18] Kuna, S. L. ., & Prasad, A. K. . (2023). Deep Learning Empowered Diabetic Retinopathy Detection and Classification using Retinal Fundus Images. International Journal on Recent and Innovation Trends in Computing and Communication, 11(1), 117–127. https://doi.org/10.17762/ijritcc.v11i1.6058